The Meteoritical Society

Meteoritics & Planetary Science 44, Nr 6, 925–940 (2009)
Abstract available online at http://meteoritics.org

Systematic study of universal-stage measurements of planar deformation features in shocked quartz: Implications for statistical significance and representation of results

Ludovic FERRIÈRE[1†*], Jared R. MORROW[2], Tsolmon AMGAA[1], and Christian KOEBERL[1]

[1]Department of Lithospheric Research, University of Vienna, Althanstrasse 14, A-1090 Vienna, Austria
[2]Department of Geological Sciences, San Diego State University, 5500 Campanile Drive, San Diego, California 92182–1020, USA
[†]Present address: Department of Earth Sciences, University of Western Ontario,
1151 Richmond Street, London, ON N6A 5B7, Canada
[*]Corresponding author. E-mail: ludovic.ferriere@uwo.ca

Supplemental material is available online at http://meteoritics.org/Online%20Supplements.htm

(Received 06 September 2008; revision accepted 04 April 2009)

Abstract–The presence of shocked quartz is one of the key lines of evidence for the impact origin of rocks. Crystallographic orientations of planar deformation feature (PDF) sets in shocked quartz have been used to constrain the peak shock pressure that these grains have experienced. So far no systematic and comparative studies of the various orientation measurement methods and their biases are available. Therefore, three shocked-quartz-bearing thin sections from a meta-greywacke clast in breccia, a biotite-gneiss, and a sandstone, respectively, were independently analyzed by three operators (two experienced and one inexperienced) using a four-axis universal-stage (U-stage), in order to evaluate the quality, precision, repeatability, and representativeness of U-stage measurements. Based on the indexing of PDF sets using a new version of the commonly used stereographic projection template, the study of 1751 PDF set orientations in 666 quartz grains in three different shocked rocks shows that differences in abundance and orientation of various PDF sets, as measured by the three separate operators, are rather limited.

The precision of U-stage measurements depends mainly on the number of PDF sets investigated, as the ability level of the operator (experienced versus inexperienced) is only responsible for minor deviations in the number of unindexed planes. The frequency percent of dominant PDF planes may vary by up to 20 percentage points (pp) or 81% for a given crystallographic orientation when only 25 sets are measured. When 100 PDF sets are measured, however, this deviation in dominant orientations is reduced to about 7 pp or 28%. We recommend the use of a new stereographic projection template, which plots the pole positions of five additional, commonly occurring PDF orientations, as it can allow indexing of up to 12 pp more PDF planes; these are planes that would previously be considered unindexed and potentially regarded as errors of measurement.

Our results suggest that by following a strict measurement procedure, the reproducibility of U-stage measurements is good and the results of different studies can be readily compared. However, it is critical that published PDF orientation histograms clearly define what type of frequency measurement is used, whether or not unindexed PDF sets are included in the frequency calculations, the numbers of grains and sets analyzed, and the relative proportions of each PDF set population that are combined in the histograms. This information appears to be essential for effectively comparing datasets from different studies.

INTRODUCTION

Universal-stage (U-stage) microscope analysis is a standard technique used for determining the crystallographic orientations of planar deformation features (PDFs) in quartz. Detection of these shock-metamorphic features and the distribution of their orientations in quartz are crucial diagnostic evidence for proving the impact origin of geological structures. Because specific crystallographic orientations of PDFs are formed at different shock pressures (e.g., Hörz 1968; Müller and Défourneaux 1968; Huffman and Reimold 1996), average shock pressure values for a given sample can be calculated on the basis of proportions of the different PDF orientations, as determined by U-stage

measurements (the method of calculation is described in the "Discussion" section below).

Upon shock compression, quartz develops irregular fractures (which are not diagnostic shock effects) and regular planar microstructures, as planar fractures (PFs) and PDFs, (e.g., French and Short 1968; Engelhardt and Bertsch 1969; Alexopoulos et al. 1988; Stöffler and Langenhorst 1994; Grieve et al. 1996; French 1998). Planar fractures are parallel open fissures with a typical spacing of more than 15–20 μm apart. They occur frequently in shocked quartz, but are not considered shock-diagnostic when occurring without accompanying PDFs. Planar fractures differ from PDFs, which are commonly composed of narrow, individual planar features of amorphous material that are less than 2 μm thick, comprising straight, parallel sets spaced 2–10 μm apart (e.g., Engelhardt and Bertsch 1969; Stöffler and Langenhorst 1994). Both PFs and PDFs are oriented parallel to rational crystallographic planes of low Miller indices ("low" refers to the Miller indices being small numbers; see Table 1). Miller indices consist of three numbers (*hkl*) representing the inverse of axial unit distances of the plane intercepts along each of the crystallographic axes (a, b, and c axes, respectively). In the case of the hexagonal crystal system (as for quartz), four numbers (*hkil*), the so-called Miller-Bravais indices, are used. These numbers represent the inverse plane intercepts along the a_1, a_2, a_3, and c axes, respectively (see, e.g., Bloss 1971). The combination of these three, or four, numbers uniquely identifies the three-dimensional orientation of planes in a crystal. The notation {*hkil*} denotes all planes that are equivalent to (*hkil*) by the symmetry of the crystal. For commonly formed orientations of planar microstructures in shocked quartz, a symbol (c, ω, π, etc.) can be substituted for, or used in conjunction with, the Miller-Bravais notation (Table 1; e.g., Stöffler and Langenhorst 1994; Langenhorst 2002).

Previous studies have shown that PFs are usually oriented parallel to (0001) and {10$\bar{1}$1}, and occasionally to {10$\bar{1}$3}, whereas PDFs are parallel commonly to {10$\bar{1}$3}, {10$\bar{1}$2}, (0001), {10$\bar{1}$1}, {11$\bar{2}$2}, {11$\bar{2}$1}, {21$\bar{3}$1}, {51$\bar{6}$1}, {10$\bar{1}$0}, and {11$\bar{2}$0}, and more rarely to other planes listed in Table 1 (e.g., Stöffler and Langenhorst 1994). The measurement of PDF orientations is possible using transmission electron microscopy (TEM; e.g., Goltrant et al. 1991), and with a spindle stage (e.g., Bohor et al. 1987), but only the U-stage technique allows a large number of PDF sets to be measured and potentially indexed efficiently and inexpensively.

Universal-stage measurements have been performed in impact geology for about 40 years; however, the quality, precision, repeatability, and representativeness of the measurements (in terms of personal and laboratory biases) for a given sample have not been thoroughly tested. For these reasons, three shocked-quartz-bearing thin sections (BOS-3, a meta-greywacke clast in polymict lithic breccia from the Bosumtwi impact structure; M8-427.7, a biotite-gneiss from the Manson impact structure; and AUS-90-43-2, a sandstone from the Gosses Bluff structure) were independently analyzed by three operators (two experienced and one inexperienced) using a four-axis U-stage mounted on an optical microscope.

This paper presents the results of this statistical analysis, based on the indexing of PDF planes using a new version of the commonly used stereographic projection template. The measurements obtained on the same three thin sections by three operators are compared, allowing discussion of the statistical meaning and reproducibility of U-stage measurements. These results expand on preliminary data reported in abstract form by Ferrière et al. (2008).

EXPERIMENTAL METHODS AND PRESENTATION OF THE MEASUREMENTS

Prior to describing our measurements, it is necessary to briefly review the method of measuring PDF orientations using the U-stage microscope, as well as discussing some definitions and the plotting and representation of data. Determination of the crystallographic orientations of PDFs in quartz grains with a U-stage microscope (see, e.g., Reinhard 1931 and Emmons 1943 for general information) is done in four main steps: (1) determination of the optic or c-axis of the grain studied; (2) measurement of the poles perpendicular to planes of all PDFs visible in the grain investigated; (3) plotting, on a stereographic Wulff net, the optic axis and poles to all PDF planes; and (4) indexing, where possible, the planes measured using a standard stereographic projection template (SPT), which displays the possible pole orientations of common PDF planes within a 5° envelope of measurement error (e.g., Engelhardt and Bertsch 1969; Stöffler and Langenhorst 1994; Grieve et al. 1996; Langenhorst 2002).

This conventional method has been used for about 40 years and was also used for our investigations. However, the SPT (as reported in, e.g., Engelhardt and Bertsch 1969; Stöffler and Langenhorst 1994), which allows the indexing of ten typical PDF crystallographic orientations in quartz, is modified herein. As shown in Table 1, five other characteristic crystallographic orientations of PDFs in quartz, which have been identified but do not appear in the commonly used SPT, are {22$\bar{4}$1}, {31$\bar{4}$1}, t{40$\bar{4}$1}, k{51$\bar{6}$0}, and {10$\bar{1}$4}. For this reason, a new version of the stereographic projection template (denoted NSPT; available online at http://meteoritics.org/Online%20Supplements.htm) that includes these additional orientations is presented (Fig. 1). As in previous versions of the SPT, the additional orientations in the NSPT are depicted as poles to PDF planes within a 5° envelope of error (Fig. 1). Note that the {10$\bar{1}$4} orientation has been added to the NSPT during the revision of the manuscript and, for comparison, only the measurements of the first "experienced operator" (see below) were re-plotted, showing the slight changes induced by the addition to the NSPT of this characteristic crystallographic orientation of PDFs. A comparison of the results as obtained using the

Table 1. Typical crystallographic orientations of planar deformation features in shocked quartz.

#	Symbol	Miller-Bravais indices {*hkil*}	Polar angle (°)*	Azimuthal angle (°)	Crystallographic form	No. of symmetrically equivalent planes
1	c	(0001)	0.00	–	Basal pinacoid	1
2	ω, ω’	{10$\bar{1}$3}, {01$\bar{1}$3}	22.95	30	Rhombohedron	3
3	Π, Π’	{10$\bar{1}$2}, {01$\bar{1}$2 }	32.42	30	Rhombohedron	3
4	r, z	{10$\bar{1}$1}, {01$\bar{1}$1}	51.79	30	Rhombohedron	3
5	m	{10$\bar{1}$0}	90.00	30	Hexagonal prism	3
6	ξ	{11$\bar{2}$2}, {2$\bar{1}\bar{1}$2}	47.73	60	Trigonal dipyramid	3
7	s	{11$\bar{2}$1}, {2$\bar{1}\bar{1}$1}	65.56	60	Trigonal dipyramid	3
8	–	{21$\bar{3}$1}, {3$\bar{2}\bar{1}$1}, {3$\bar{1}$2$\bar{1}$}, {12$\bar{3}$1}	73.71	50	Trigonal trapezohedron	6
9	x	{51$\bar{6}$1}, {6$\bar{5}\bar{1}$1}, {6$\bar{1}$5$\bar{1}$}, {15$\bar{6}$1}	82.07	40	Trigonal trapezohedron	6
10	a	{11$\bar{2}$0}, {2$\bar{1}\bar{1}$0}	90.00	60	Trigonal prism	3
11	–	{22$\bar{4}$1}, {4$\bar{2}\bar{2}$1}	77.20	60	Trigonal dipyramid	3
12	–	{31$\bar{4}$1}, {4$\bar{3}\bar{1}$1}, {4$\bar{1}$3$\bar{1}$}, {13$\bar{4}$1}	77.91	45	Trigonal trapezohedron	6
13	t	{40$\bar{4}$1}, {04$\bar{4}$1}	78.87	30	Rhombohedron	3
14	k	{51$\bar{6}$0}, {6$\bar{1}$5$\bar{0}$}	90.00	40	Ditrigonal prism	6
e	–	{10$\bar{1}$4}, {01$\bar{1}$4}	17.62	30	Rhombohedron	3

Data modified from Stöffler and Langenhorst (1994).

*Angle between the poles to the planar deformation features and the c-axis of quartz.

Table 2. Locations and petrographic descriptions of the investigated samples.

	Meta-greywacke (clast in polymict lithic breccia)	Biotite-gneiss	Sandstone (Carmichael sandstone)
Sample	BOS-3	M8-427.7	AUS-90-43-2
Structure name	Bosumtwi, Ghana	Manson, Iowa, USA	Gosses Bluff, Australia
Location	Drill core LB-07A; Deep crater moat; Depth: 341.5 m (see Morrow 2007)	Drill core M8; Eastern slope of the central uplift; Depth: 427.7 ft (129.6 m) (see Koeberl et al. 1996)	From rim of the central uplift ring
Description	Fine-grained meta-greywacke mainly composed of quartz, feldspar, muscovite, chlorite, and biotite. Quartz grains show planar fractures (PFs), planar deformation features (PDFs), and mosaicism. Numerous PDFs are strongly decorated with tiny fluid inclusions. Many quartz grains are toasted. Extremely rare PDFs occur in feldspar.	Well-foliated gneiss composed mainly of quartz, feldspar, biotite, muscovite, and rare opaque minerals. Quartz and feldspar display numerous PDFs. Rare quartz grains show mosaicism. Numerous PDFs in quartz grains are decorated. Most of the quartz grains are toasted. Biotite shows kinkbanding.	Medium-grained sandstone composed of subrounded to subangular quartz grains. Numerous quartz grains display undulatory extinction. Most of the grains show PFs and/or PDFs. The planar microstructures are rarely decorated. A few grains are slightly toasted.

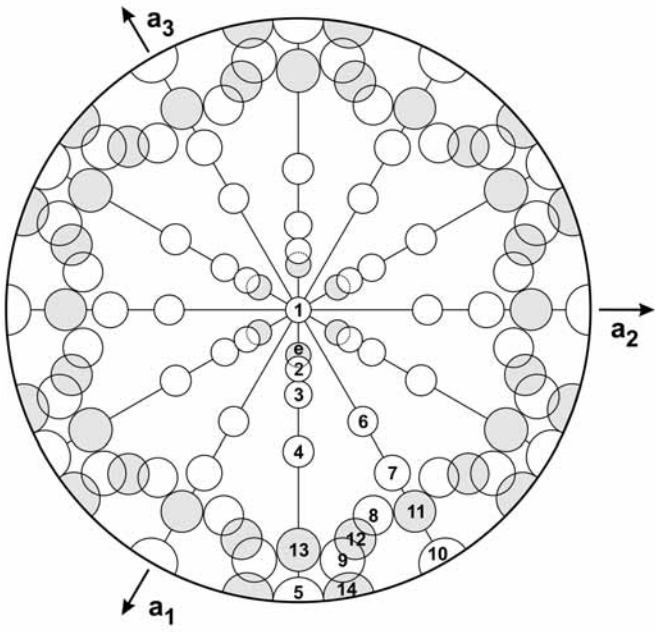

Plane	Pole angle to c-axis				
1 (0001)	0.00°	6 {11$\bar{2}$2}	47.73°	11 {22$\bar{4}$1}	77.20°
2 {10$\bar{1}$3}	22.95°	7 {11$\bar{2}$1}	65.56°	12 {31$\bar{4}$1}	77.91°
3 {10$\bar{1}$2}	32.42°	8 {21$\bar{3}$1}	73.71°	13 {40$\bar{4}$1}	78.87°
4 {10$\bar{1}$1}	51.79°	9 {51$\bar{6}$1}	82.07°	14 {51$\bar{6}$0}	90.00°
5 {10$\bar{1}$0}	90.00°	10 {11$\bar{2}$0}	90.00°	e {10$\bar{1}$4}	17.62°

Fig. 1. New stereographic projection template (NSPT) used in this study. This is based on the standard stereographic projection of quartz with the c-axis plotted in the center. Each circle (5° radius) marks the position of the most common poles to PDF planes. Modified from the previously used stereographic project template, e.g., Stöffler and Langenhorst (1994) and Langenhorst (2002); four additional high-index PDF orientations (Planes #11–14) are also indicated (gray circles), as well as the {10$\bar{1}$4} orientation (marked by "e" in the template), which partially overlaps the 5° envelope of the {10$\bar{1}$3} PDFs pole traces.

different versions of the stereographic projection template is provided in the discussion part, and the overlaps of the 5° error envelope of some of the PDFs pole traces, as visible on Fig. 1, are also discussed.

In the present study, each operator received a stereographic Wulff net, the NSPT (at the time without the {10$\bar{1}$4} orientation), a formatted Excel spreadsheet, and a standardized set of instructions. Operators were asked to determine, following conventional measurement methods (described above), the crystallographic orientations of a maximum number of measurable PDFs, where possible excluding PFs, contained within ~50–100 quartz grains in each thin section. In addition, the analyses were "blind," in that each operator selected grains without prior knowledge of the specific grains measured by the other workers. Each operator was instructed to plot the PDF orientations manually on the stereographic Wulff net, and then to index the planes

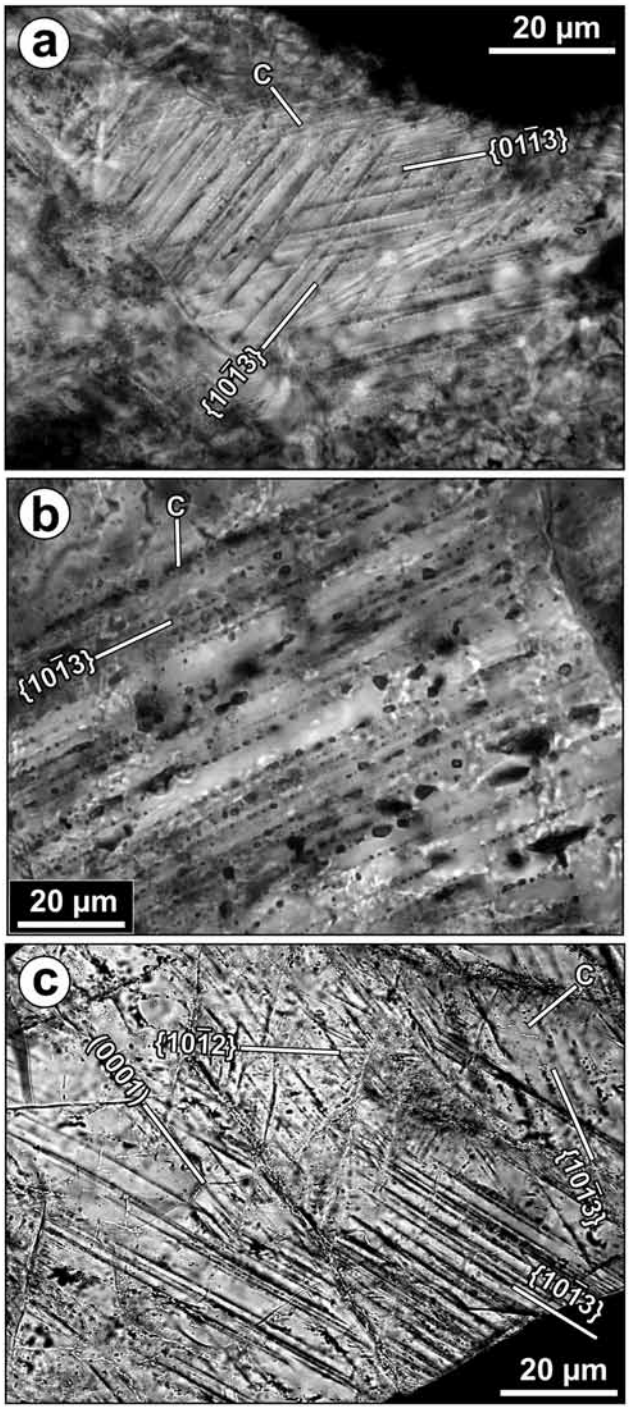

Fig. 2. a) Thin section photomicrograph of quartz grain containing two prominent decorated PDF sets with ω{10$\bar{1}$3}- and ω'{01$\bar{1}$3}-equivalent orientations. Quartz c-axis is indicated. Sample BOS-3, plane-polarized light. b) Thin section photomicrograph of quartz grain containing one decorated PDF set with ω{10$\bar{1}$3}-equivalent orientation. Quartz c-axis is indicated. Sample M8-427.7, plane-polarized light. c) Thin section photomicrograph of highly shocked quartz grain with at least four orientations of relatively non-decorated planar microstructures, including c(0001), ω{10$\bar{1}$3}, and π{10$\bar{1}$2} PDF sets and a second, ω{10$\bar{1}$3}-equivalent PF set. Quartz c-axis is indicated. Sample AUS-90-43-2, cross-polarized light.

with Miller-Bravais indices {*hkil*} for quartz using the NSPT. To allow a detailed statistical evaluation, each operator reported the stereonet-determined polar angle values between the quartz c-axis and poles to the planes of PDFs, as well as the assigned specific Miller-Bravais indices for each set measured, in an Excel spreadsheet. All data were then compiled, recalculated, and plotted by the lead author.

U-stage measurement data are commonly reported in publications using two different types of histograms: one where the number (or frequency) of uncorrected polar angle values are plotted into bins of 2–5°, or a second one where polar angle values are uniquely indexed within a 5° range of error and assigned to specific crystallographic indices (see, e.g., Grieve et al. 1996 for discussion). Frequently, no information is given on the exact methodology used for the measurements, how the data were recalculated, the number of sets measured, etc. In addition, tables including the raw data used to construct histograms are mostly not included. However, for understanding the quality of the data, it is critical that published PDF orientation histograms clearly define which version of frequency measurement is used (i.e., relative or absolute frequency; Engelhardt and Bertsch 1969), whether or not unindexed PDF sets are included in the frequency calculations, and the total numbers of grains and sets used in the calculations.

The definition of the relative and absolute frequency of PDF orientations is given by Engelhardt and Bertsch (1969) and clarified by D. Stöffler (written commun. 2008):

$$\text{relative frequency } f_{hkil} = q_{hkil} / p_{hkil} \times 100\ (\%)$$

$$\text{absolute frequency } F_{hkil} = q_{hkil} / Q \times 100\ (\%)$$

where q_{hkil} is the actual number of symmetrically equivalent planes observed in *n* quartz grains, p_{hkil} the maximum number of symmetrically equivalent planes potentially observable in *n* quartz grains (i.e., number of symmetrically equivalent planes multiplied by *n*, the number of measured quartz grains, see Table 1), and Q the total number of all sets of PDFs, indexed and unindexed, observed in *n* quartz grains of a thin section. It is important to note that, because of the p_{hkil} term, the total relative frequency can be much less than, or exceed, 100% (Table 1). According to these definitions, it seems that absolute frequency has been most widely used in previous published histograms, although, as noted above, this is often not specified.

SAMPLES

Three shocked-quartz-bearing thin sections of different lithologies and from different impact structures were independently investigated by each of the three operators. Petrographic characteristics of the three investigated samples, which include a meta-greywacke clast in breccia (BOS-3), a biotite-gneiss (M8-427.7), and a sandstone (AUS-90-43-2), are summarized in Table 2. The different samples were selected principally because of the abundance of PDF-bearing quartz grains in their respective thin sections and also in order to cover a wide variety of target lithologies.

In samples BOS-3 and M8-427.7, numerous PDFs in quartz are decorated with tiny fluid inclusions (Fig. 2), whereas in sample AUS-90-43-2, only non-decorated PDFs occur. This difference is potentially important, as decorated PDFs are more easily detected and measured as compared to the less visible, non-decorated PDFs. A number of quartz grains in the three samples display blocky, undulatory extinction, which can reduce the precision of the measurements because of uncertainty in the c-axis orientation. In addition, many quartz grains in samples BOS-3 and M8-427.7 have a grayish-brown appearance in plane-polarized light, with patches containing micrometer-scale fluid inclusions; these quartz grains have been described as "toasted" (Short and Gold 1996; Whitehead et al. 2002). In some cases, PDFs are partially masked in toasted quartz grains and are difficult to discern and measure.

RESULTS AND DISCUSSION

The crystallographic orientations of 1751 PDF sets in 666 quartz grains were measured on three thin sections, one section each from samples BOS-3, M8-427.7, and AUS-90-43-2 (Table 3). For comparison, results are reported in both relative and absolute frequency. Histograms showing the proportion of angles, binned at 5°, between the c-axis and poles to PDF planes in quartz grains from the three samples, as determined by each of the three operators, are shown in Fig. 3. The unindexed plane sets, which could not be assigned using the NSPT (without the $\{10\bar{1}4\}$ orientation), are also reported in Fig. 3 in order to evaluate whether they show a preferred range of orientations. Usually, unindexed PDF orientations are considered to be the result of measurement or plotting errors (e.g., Langenhorst 2002) and they are normally ignored and rarely discussed. However, in several cases as observed by the two experienced operators, some of the unindexed plane sets are undoubtedly PDFs that cannot be indexed, even if the measurement and plotting operation is repeated several times. We have noted that the poles to the unindexed PDF planes principally have angles of 10–30° to the c-axis (Fig. 3). Therefore, the addition to the stereographic projection template of the $\{10\bar{1}4\}$ orientation allows indexing of PDF planes with angles of about 18° (see Table 4 and discussion below). Additional examination of the unindexed PDFs, e.g., using TEM techniques, is warranted, as the $\{10\bar{1}4\}$ orientation was characterized in some shocked quartz grains using TEM (see Goltrant et al. 1991, 1992). In addition, this orientation has been recognized routinely by researchers from the former Soviet Union (see, e.g., Gurov and Gurova 1991; Gurov et al. 2005).

Table 3. Summary of PDF set abundances and indexed PDF crystallographic orientations in quartz grains from BOS-3, M8-427.7, and AUS-90-43-2, as determined using the universal-stage by three operators, two experienced (1, 2) and one inexperienced (3).

	BOS-3			M8-427.7			AUS-90-43-2		
Operator	1	2	3	1	2	3	1	2	3
No. of investigated grains	65	100	49	71	100	52	74	100	55
No. of measured sets	145	198	127	212	262	156	208	267	176
No. of PDF sets/grain (N)	2.2	2.0	2.6	3.0	2.6	3.0	2.8	2.7	3.2
No. of PDF sets/grain (N^*)[a]	2.1	1.8	2.3	2.8	2.4	2.5	2.6	2.5	2.9
PDF sets; % relative to total no. of quartz grains examined									
1 set	23	28	14	8.5	11	1.9	19	6.0	15
2 sets	42	49	43	24	37	31	26	41	22
3 sets	26	20	24	35	34	42	27	37	25
4 sets	7.7	3.0	8.2	27	15	17	16	13	20
5 sets	1.5	n.d.	8.2	4.2	3.0	5.8	9.5	2.0	7.3
6 sets	n.d.	n.d.	2.0	1.4	n.d.	1.9	1.4	1.0	9.1
7 sets	n.d.	n.d.	n.d.	n.d.	n.d.	n.d.	1.4	n.d.	n.d.
8 sets	n.d.	n.d.	n.d.	n.d.	n.d.	n.d.	n.d.	n.d.	1.8
Total	100	100	100	100	100	100	100	100	100
Indexed PDF crystallographic orientations; absolute frequency (%)[b]									
PDF crystallographic orientations									
c (0001)	n.d.	2.5	n.d.	1.9	1.1	0.6	28	22	22
ω {10$\bar{1}$3}	54	48	51	73	67	68	50	51	51
Π {10$\bar{1}$2}	19	19	20	0.9	5.7	3.8	1.0	7.9	4.0
r, z {10$\bar{1}$1}	3.4	4.5	4.7	6.1	5.7	3.8	4.8	2.2	9.1
m {10$\bar{1}$0}	0.7	0.5	0.8	n.d.	0.4	n.d.	0.5	n.d.	n.d.
ξ {11$\bar{2}$2}	2.8	3.0	0.8	1.4	4.6	1.9	2.4	4.5	0.6
s {11$\bar{2}$1}	1.4	4.5	2.4	n.d.	1.1	0.6	n.d.	1.1	0.6
ρ {21$\bar{3}$1}	2.1	4.5	0.8	1.4	1.9	2.6	1.4	0.7	1.1
x {51$\bar{6}$1}	0.7	2.0	1.6	0.5	1.9	0.6	0.5	0.4	n.d.
a {11$\bar{2}$0}	0.7	1.0	n.d.	n.d.	0.8	n.d.	0.5	n.d.	n.d.
{22$\bar{4}$1}	4.1	1.0	3.9	4.7	n.d.	1.9	n.d.	2.2	1.7
{31$\bar{4}$1}	2.1	1.0	1.6	0.9	0.8	n.d.	1.4	n.d.	n.d.
t {40$\bar{4}$1}	1.4	0.5	0.8	0.9	0.8	0.6	1.0	n.d.	1.1
k {51$\bar{6}$0}	n.d.	n.d.	n.d.	0.5	0.4	n.d.	0.5	n.d.	n.d.
Unindexed	6.9	7.6	11.8	7.5	8.0	15.4	7.7	7.5	8.5
Total	100	100	100	100	100	100	100	100	100
Indexed PDF crystallographic orientations; relative frequency (%)[b]									
PDF crystallographic orientations									
c (0001)	n.d.	5.0	n.d.	5.6	3.0	1.9	80	60	71
ω {10$\bar{1}$3}	41	32	44	73	58	68	47	45	55
Π {10$\bar{1}$2}	14	13	17	0.9	5.0	3.8	0.9	7.0	4.2
r, z {10$\bar{1}$1}	2.6	3.0	4.1	6.1	5.0	3.8	4.5	2.0	9.7
m {10$\bar{1}$0}	0.5	0.3	0.7	n.d.	0.3	n.d.	0.5	n.d.	n.d.
ξ {11$\bar{2}$2}	2.1	2.0	0.7	1.4	4.0	1.9	2.3	4.0	0.6
s {11$\bar{2}$1}	1.0	3.0	2.0	n.d.	1.0	0.6	n.d.	1.0	0.6
ρ {21$\bar{3}$1}	0.8	1.5	0.3	0.7	0.8	1.3	0.7	0.3	0.6
x {51$\bar{6}$1}	0.3	0.7	0.7	0.2	0.8	0.3	0.2	0.2	n.d.
a {11$\bar{2}$0}	0.5	0.7	n.d.	n.d.	0.7	n.d.	0.5	n.d.	n.d.
{22$\bar{4}$1}	3.1	0.7	3.4	4.7	n.d.	1.9	n.d.	2.0	1.8
{31$\bar{4}$1}	0.8	0.3	0.7	0.5	0.3	n.d.	0.7	n.d.	n.d.
t {40$\bar{4}$1}	1.0	0.3	0.7	0.9	0.7	0.6	0.9	n.d.	1.2
k {51$\bar{6}$0}	n.d.	n.d.	n.d.	0.2	0.2	n.d.	0.2	n.d.	n.d.
Total	67	62	74	94	80	84	138	122	144

[a]Calculated only on indexed sets (i.e., unindexed sets excluded).

[b]Method described in, e.g., Engelhardt and Bertsch (1969) and Stöffler and Langenhorst (1994).

n.d. = none detected.

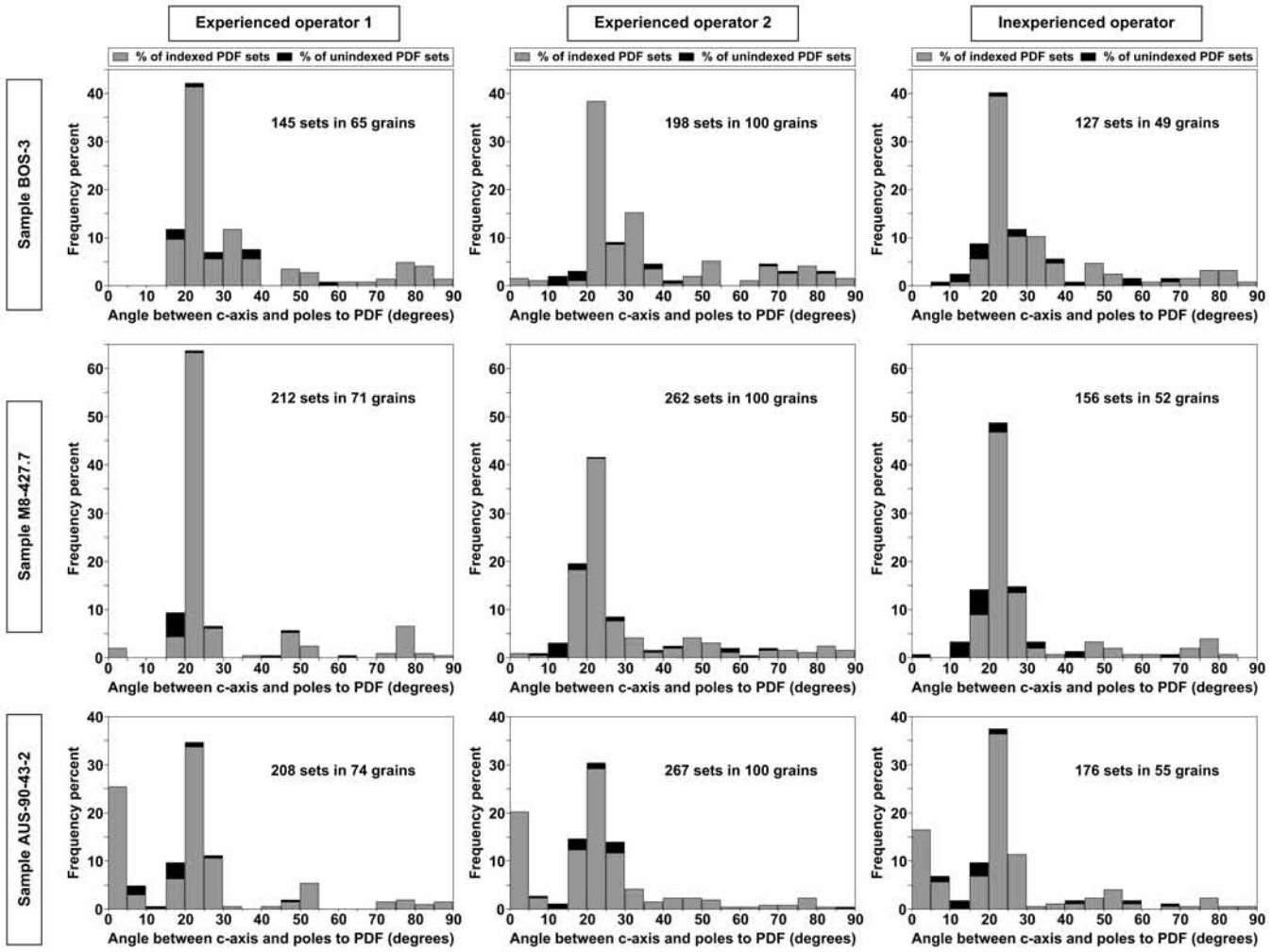

Fig. 3. Histograms of angles between c-axis and poles to PDF, binned by 5°, in quartz grains from samples BOS-3, M8-427.7, and AUS-90-43-2, as determined by the three operators, two experienced and one inexperienced. All measured PDF orientations are reported; "indexed" and "unindexed" portions of the histogram bars are based on measurements using the NSPT (without the $\{10\bar{1}4\}$ orientation). Note that the unindexed PDF orientations (in black) are mainly concentrated with angles of 10–30° between c-axis and poles to PDFs.

As reported in Table 3, the proportion of unindexed planes is nearly identical for the two experienced operators, at 7–8% for the three thin sections investigated (using the NSPT without the $\{10\bar{1}4\}$ orientation), whereas this proportion is variable for the inexperienced operator, ranging from 8.5–15.5%. It is evident that observer ability had an influence on the resulting number of unindexed planes.

To allow consistent comparison of results, the data were recalculated to 100% without including unindexed PDF orientations in order to prevent the skewing of plane distributions. Histograms of the absolute frequency percent of indexed PDF sets versus angle between the c-axis and poles to PDF planes for the three samples, as determined by the different operators, are shown in Fig. 4. The three samples have noticeably different distributions of PDF orientations: the dominant PDF orientations (>10–15 absolute frequency percent) are $\{10\bar{1}3\}$ and $\{10\bar{1}2\}$ for sample BOS-3; $\{10\bar{1}3\}$ for M8-427.7; and (0001) and $\{10\bar{1}3\}$ for AUS-90-43-2 (Fig. 4). Planes parallel to the $\{10\bar{1}1\}$, $\{11\bar{2}2\}$, $\{11\bar{2}1\}$, $\{21\bar{3}1\}$, $\{51\bar{6}1\}$, $\{22\bar{4}1\}$, $\{31\bar{4}1\}$, $\{40\bar{4}1\}$, $\{10\bar{1}0\}$, $\{11\bar{2}0\}$, and $\{51\bar{6}0\}$ orientations are also present (Table 3; Fig. 4), but in lower proportions.

Surprisingly, no major difference in distribution of PDF orientations occurs from operator to operator; the average standard deviation of the orientation measurements between the three operators is between 1.2% and 1.4% for the three samples, with a maximum standard deviation of 4.1% for the $\{10\bar{1}3\}$-equivalent crystallographic orientation in sample M8-427.7 (Fig. 4). It is important to note that a large number of PDFs sets were measured by each operator (between 127 and 267 for each thin section), which is not the case in many previous studies, where generally <50 and sometimes <20 PDF sets were measured.

Our study also shows that the average number of PDF sets per grain in a sample (denoted N; including all measured PDF orientations, both indexed and unindexed) varies from

Table 4. Summary of indexed PDF crystallographic orientations (absolute frequency, %), as determined using the universal -stage by one operator (i.e., experienced operator 1), in quartz grains from BOS-3, M8-427.7, and AUS-90-43-2, and using three different versions of stereographic projection template for the indexing.

PDF crystallographic orientations	BOS-3			M8-427.7			AUS-90-43-2		
	A[a]	*B*[b]	*C*[c]	*A*	*B*	*C*	*A*	*B*	*C*
c (0001)	n.d.	n.d.	n.d.	1.9	1.9	1.9	28	28	28
{10$\bar{1}$4}	n.a.	n.a.	1.4	n.a.	n.a.	5.2	n.a.	n.a.	2.9
{10$\bar{1}$4} // {10$\bar{1}$3}[d]	n.a.	n.a.	32	n.a.	n.a.	36	n.a.	n.a.	21
ω {10$\bar{1}$3}[e]	54	54	22	73	73	37	50	50	29
Π {10$\bar{1}$2}	19	19	19	0.9	0.9	0.9	1.0	1.0	1.0
r, z {10$\bar{1}$1}	3.4	3.4	3.4	6.1	6.1	6.1	4.8	4.8	4.8
m {10$\bar{1}$0}	0.7	0.7	0.7	n.d.	n.d.	n.d.	0.5	0.5	0.5
ξ {11$\bar{2}$2}	2.8	2.8	2.8	1.4	1.4	1.4	2.4	2.4	2.4
s {11$\bar{2}$1}	1.4	1.4	1.4	n.d.	n.d.	n.d.	n.d.	n.d.	n.d.
ρ {21$\bar{3}$1}	2.1	2.1	2.1	1.4	1.4	1.4	1.4	1.4	1.4
x {51$\bar{6}$1}	0.7	0.7	0.7	0.5	0.5	0.5	0.5	0.5	0.5
a {11$\bar{2}$0}	0.7	0.7	0.7	n.d.	n.d.	n.d.	0.5	0.5	0.5
{22$\bar{4}$1}	n.a.	4.1	4.1	n.a.	4.7	4.7	n.a.	n.d.	n.d.
{31$\bar{4}$1}	n.a.	2.1	2.1	n.a.	0.9	0.9	n.a.	1.4	1.4
t {40$\bar{4}$1}	n.a.	1.4	1.4	n.a.	0.9	0.9	n.a.	1.0	1.0
k {51$\bar{6}$0}	n.a.	n.d.	n.d.	n.a.	0.5	0.5	n.a.	0.5	0.5
Unindexed	14.5	6.9	5.5	14.6	7.5	2.4	10.6	7.7	4.8
Total	100	100	100	100	100	100	100	100	100

[a]PDF planes indexed using the STP; as reported in Engelhardt and Bertsch (1969) and in Stöffler and Langenhorst (1994).
[b]PDF planes indexed using the NSTP; without the {10$\bar{1}$4} crystallographic orientation.
[c]PDF planes indexed using the NSTP; including the {10$\bar{1}$4} crystallographic orientation (cf. Fig. 1).
[d]PDF planes which plot in the overlapping zone between {10$\bar{1}$4} and {10$\bar{1}$3} crystallographic orientations.
[e]{10$\bar{1}$3} PDF orientations uniquely indexed.
n.d. = none detected. n.a. = not applicable.

operator to operator, even though the same thin sections were investigated (Figs. 4–5; Table 3). Interestingly, the difference in the N values between the operators is nearly constant for each thin section (Fig. 5). However, this difference does not seem to be directly influenced by observer experience. The total number of grains measured can influence N in the case of non-homogeneously shocked rock; an unintentional "selection" of the more heavily shocked grains can be another explanation.

With respect to the comparison of datasets from different studies and from different investigators, we have introduced a new term, "N*" (Fig. 4; Table 3), which is defined as the average number of indexed PDF sets per grain in a sample, where unindexed PDF orientations are excluded from the calculations. Values of N* are lower than values of N for any given sample (Table 3), but trends are similar.

Regarding the number of measured PDF sets within individual grains (i.e., 1–8 sets per grain in this study), some inter-operator differences are noticed (Fig. 6; Table 3). For the experienced operators, a more or less "normal distribution" of the different PDF set abundances is observed, whereas a somewhat "bimodal distribution" is seen for the inexperienced operator. As noted for the values of N or N*, the proportions of the different PDF set populations are possibly influenced by the total number of grains measured, as well as by an unintentional "selection" of the grains investigated. Nevertheless, as grains with 6–8 PDF sets were almost exclusively identified and measured by the inexperienced operator, it cannot be excluded that this operator possibly measured grains with multiple crystallographic domains and considered these domains to be within a single monocrystalline grain with one c-axis, instead of within polycrystalline parts characterized by variable c-axis orientations. In most cases, these measurements, which rarely represent more than 2% of the total (see Table 3), correspond to unindexed planes, and, thus, are excluded from the statistics. Accordingly, it seems that the distribution of the PDF set abundances within a thin section should more closely correspond to a "normal distribution." Plots similar to those shown in Fig. 6 can then be used to evaluate the reliability of the U-stage measurements.

Sample Size Versus Index Distribution

Due to the limitations of the U-stage layout, usually only about one third of a thin section area can be investigated. However, as some samples contain hundreds if not thousands of grains showing PDFs, the investigator will have to stop after a certain number of measurements, having covered only part of the thin section. It is, therefore, difficult to avoid an unintentional "selection" of the grains investigated. Nevertheless, as shown in Fig. 7, in which the measured number of PDF sets per individual grain are reported in

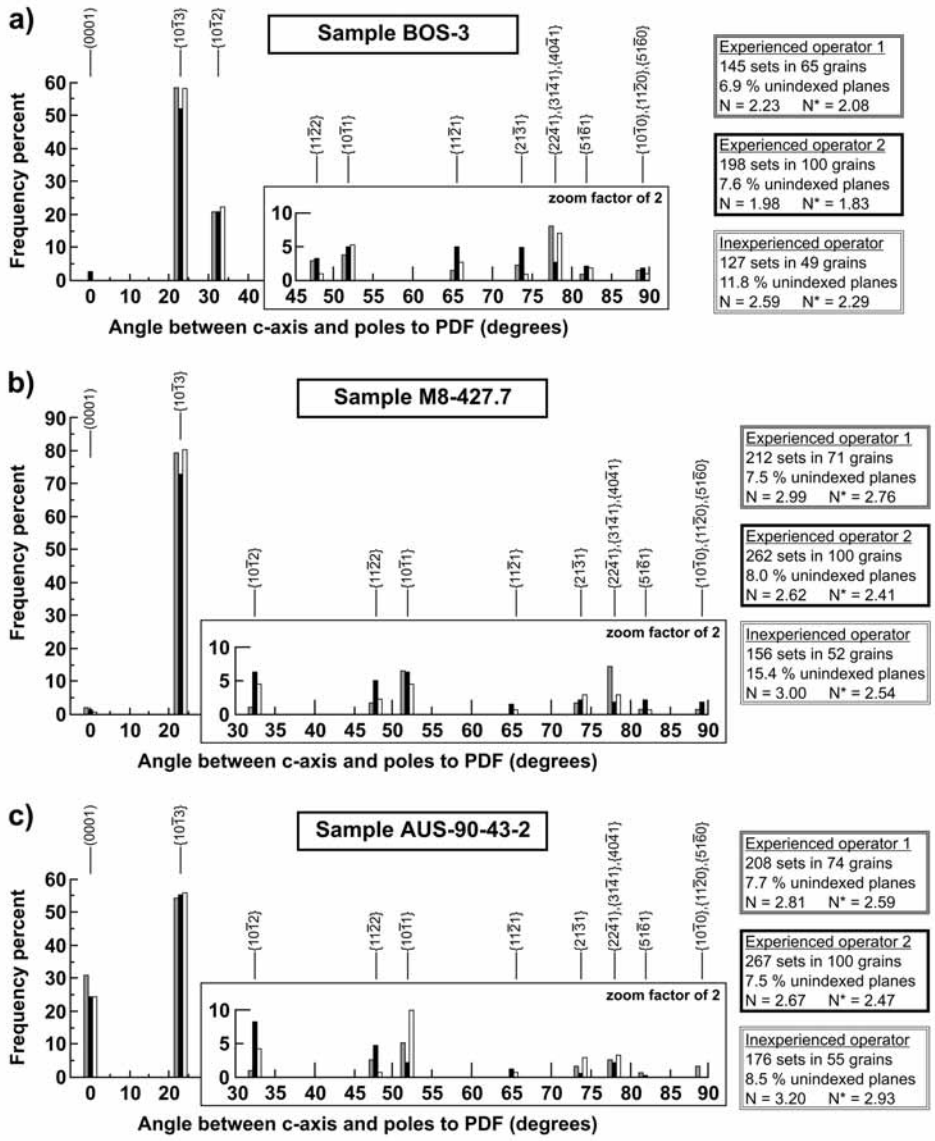

Fig. 4. Histograms of absolute frequency percent of indexed PDFs (recalculated to 100% without unindexed PDF orientations) in quartz grains from (a) BOS-3, (b) M8-427.7, and (c) AUS-90-43-2, as determined by the three operators. Recalculation without unindexed PDF orientations, which vary between operators (from 6.9–15.4%; see right column), was performed to allow consistent comparison of the datasets. The average number of PDF sets per grain (denoted N, including all measured PDF orientations, both indexed and unindexed; and N*, including indexed PDF orientations only) varies as well from operator to operator.

chronological order for each operator, a more or less "saw tooth" distribution is observed, indicating that no apparent selection bias was applied. These distribution patterns also show that the total number of grains measured may influence the reliability of the values of N or N*. Predictably, better precision is obtained through the investigation of a larger number of grains.

In order to evaluate the influence of number of grains investigated and number of PDF sets measured on the resulting distribution of the indexed PDF sets, we generated several histogram plots for each sample investigated, considering the first 25, the first 50, and the first 100 PDF sets measured (Fig. 8). For each sample, measurements of single investigators are compared to the compiled group data, which are taken as a reference. It is obvious that larger differences in the frequency percent of indexed PDF orientations occur when considering only the first 25 PDF sets measured. When using only the first 25 measurements, the frequency percent of dominant PDF planes may vary by up to 20 percentage points (pp; note that percentage points are the unit for the arithmetic difference of two percentages) or 81% between the reference and single operator values (Fig. 8). When considering the first 50 PDF sets measured, the maximum difference observed is about 12 pp or 48% for the dominant

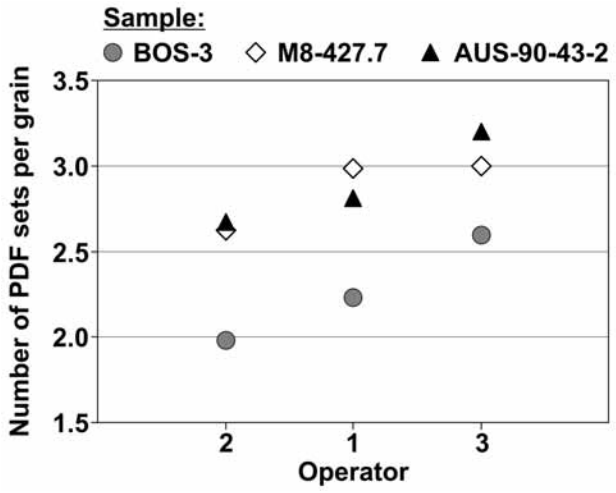

Fig. 5. Average number of PDF sets per grain (N) in the three investigated samples (BOS-3, M8-427.7, and AUS-90-43-2), as determined by the three operators, two experienced (1, 2) and one inexperienced (3). Note that the difference in the N values between the operators is of the same magnitude for each investigated thin section (see text for further discussion).

PDF orientations, and when considering the first 100 PDF sets measured, the maximum difference in dominant PDF orientations is about 7 pp or 28% (Fig. 8). Regarding the other less common PDF set orientations, which represent individually <10% of the total, the precision is even lower than for the dominant orientations. Thus, the presence or absence and abundance of these "accessory" orientations may be quite variable with smaller numbers of measurements. Based on these results, it is evident that a relationship exists between the number of PDF sets measured in a thin section and the reliability and precision of the results.

Biases Due to Methodology

We have shown that besides the dominant PDF orientations ((0001), {10$\bar{1}$3}, and {10$\bar{1}$2}), several other "accessory" PDF orientations are present (Table 3; Fig. 4). Individually, these "accessory" PDF orientations do not represent more than 10%, but in total they represent 12–25 absolute frequency percent based on our measurements using the NSPT (Fig. 1, without the {10$\bar{1}$4} orientation). The use of the NSPT (without the {10$\bar{1}$4} orientation), may allow a reduction in the proportion of unindexed PDFs by a factor of about 2; these PDF planes would have been considered as unindexed using the SPT. When using the NSPT (including the {10$\bar{1}$4} orientation), the proportion of unindexed PDFs is further reduced; i.e., from 14.6% when using the STP, to 7.5% when using the NSPT (without the {10$\bar{1}$4} orientation), and to only 2.4% when using the NSPT (including the {10$\bar{1}$4} orientation) in the case of sample M8-427.7 (see Table 4). However, unlike minor overlap of the 5° envelopes for traditional and newly added high-index PDF pole orientations, the zone of overlap between the {10$\bar{1}$4} and {10$\bar{1}$3} orientations is significant (see Fig. 1). In a similar way for the #2-14 planes (see Fig. 1), two or more sets of non-(0001) planes need to be measured in one grain with respect to index planes parallel to the {10$\bar{1}$4} orientation. But, because PDF orientations parallel to {10$\bar{1}$4} are "accessory" PDF orientations compared to the dominant {10$\bar{1}$3} PDF orientations, as suggested by TEM investigations (Goltrant et al. 1991, 1992), and because it is impossible to uniquely distinguish between {10$\bar{1}$4} and {10$\bar{1}$3} orientations using the U-stage when the angle between c-axis and poles to PDF is about 18–23°, all measured planes that fall into the overlap zone between {10$\bar{1}$4} and {10$\bar{1}$3} orientations are best considered as {10$\bar{1}$3} orientations for the purpose of U-stage analysis. Based on this assumption, between 1.4 and 5.2 absolute frequency percent of PDF orientations parallel to {10$\bar{1}$4} occur in the three investigated samples (Table 4; Fig. 9). The previous assumption is also necessary with respect to comparing future U-stage measurements with those previously reported in the literature. It is, however, recommended to include an additional row in the data table with the number/proportion of planes that plot in the overlapping zone between {10$\bar{1}$4} and {10$\bar{1}$3} orientations (as is shown in Table 4).

To evaluate the robustness of the typically used histogram, i.e., the one showing the combination of all PDF set populations, the absolute frequency of indexed PDFs was also recalculated using only measurements from quartz grains with one and two PDF sets (Fig. 10). In our study, histograms constructed from grains with three or more PDF sets are similar to those based on two sets; therefore, only histograms based on grains with two sets are shown (Fig. 10).

All histograms for both samples BOS-3 and M8-427.7 are relatively similar. However, larger variations are visible in the histograms based on one PDF set than in histograms based on two sets, when these first two plots are compared to the histograms combining all PDF set populations (Fig. 10). For sample AUS-90-43-2, the histogram based on quartz grains with only one set of PDFs is very different compared to the histograms based on grains with two sets of PDFs and on all PDF set populations. For this sample, the PDFs parallel to (0001) represent a dominant orientation, and apparently the proportion of quartz grains with one set of PDFs has an overriding influence on the combined index distribution pattern.

Based on these observations, it would seem useful to evaluate the robustness of future published PDF orientation histograms by plotting separately the measurements for the different PDF set populations. In addition to the number of investigated grains and sets, number of unindexed grains, etc., the relative proportion of each PDF set population that is combined into the published summary PDF orientation histogram should also be reported.

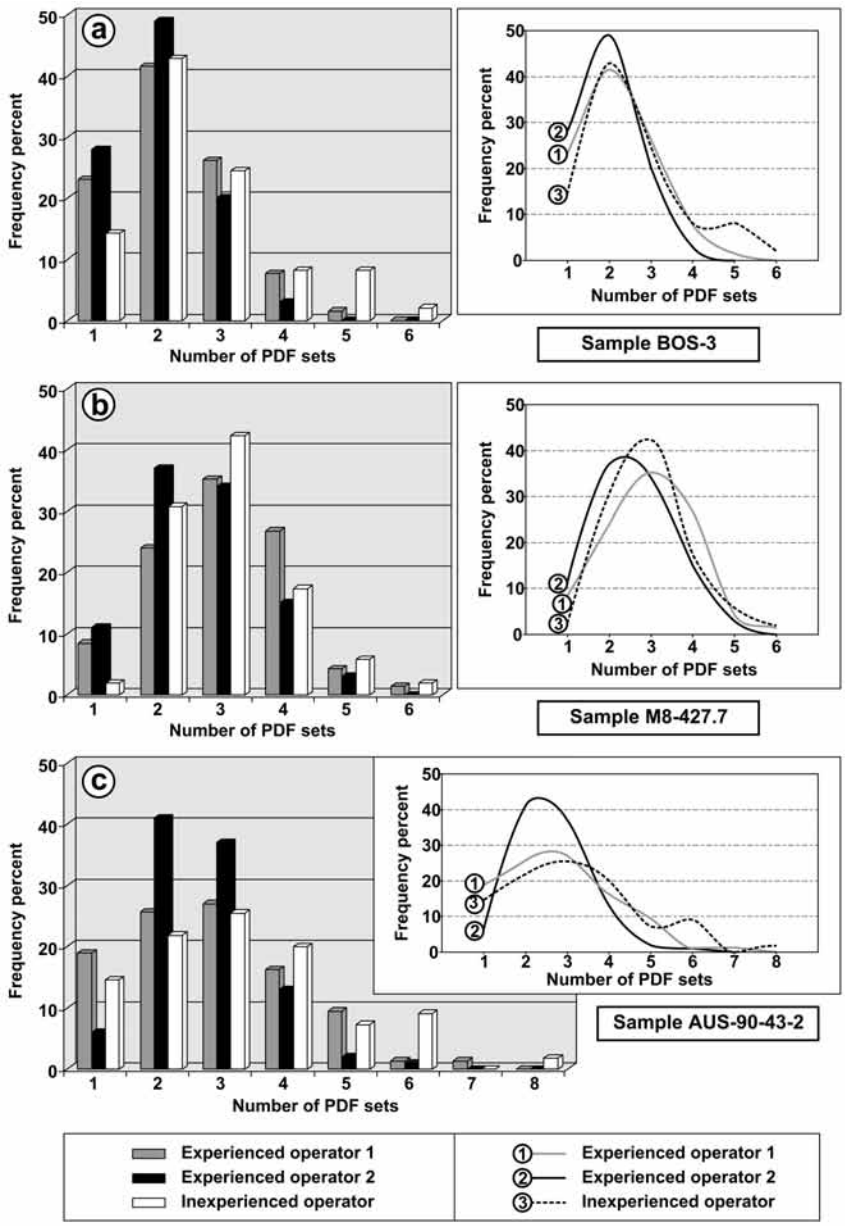

Fig. 6. Frequency distribution of the number of PDF sets for the three samples (a) BOS-3, (b) M8-427.7, and (c) AUS-90-43-2, as determined by the three operators. Note the skewness of the distribution curves for number of PDF sets in (a) and (c), and the nearly Gaussian curve in (b). The distribution, notably in (a) and (c), is somewhat "bimodal" for the inexperienced operator.

Influence on Shock Barometry

As specific orientations of PDFs in quartz are formed at different shock pressures (e.g., Hörz 1968; Müller and Défourneaux 1968; Huffman and Reimold 1996), several authors, e.g., Robertson and Grieve (1977), Grieve et al. (1990), and Dressler et al. (1998), have evaluated shock barometry using a method developed by Grieve and Robertson (1976). This method consists of the calculation of average shock pressure values for each investigated sample, based on laboratory shock experiments that bracket the pressure ranges associated with the development of individual PDF orientations or assemblages of orientations in quartz grains. For summaries of this method and references see, e.g., Stöffler and Langenhorst (1994) and Grieve et al. (1996); however, DeCarli et al. (2002) provided a cautionary discussion regarding the potential limitations of this technique. In the Grieve and Robertson (1976) study, a value of 8.8 GPa was assigned for grains with only one set of PDF orientations parallel to (0001), 12 GPa for grains with PDF orientations parallel to $\{10\bar{1}3\}$ and usually to (0001), 15 GPa for grains with PDF orientations parallel to $\{22\bar{4}1\}$ and usually to $\{10\bar{1}3\}$ and (0001), and 17.5 GPa for grains with PDF orientations parallel to $\{10\bar{1}2\}$ and usually to $\{22\bar{4}1\}$

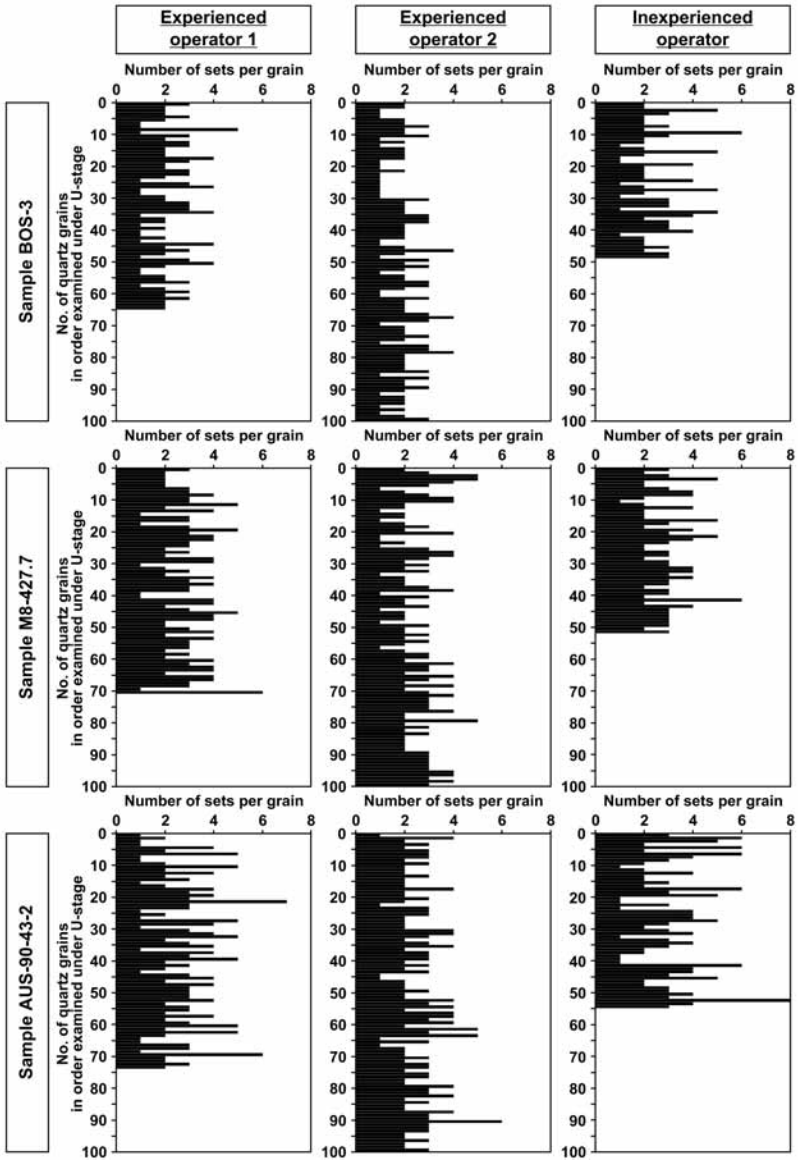

Fig. 7. Histogram suites showing the numbers of PDF sets per grain, in the order measured by each operator under the U-stage. Note that no specific concentration of quartz grains with low or high numbers of PDF sets is discernible. A more or less "saw tooth"-shaped distribution is observed.

and $\{10\bar{1}3\}$ (see Grieve and Robertson (1976) for more details on the method). In their study, the U-stage technique was used to measure the orientations of PDF sets in 14–20 grains, containing 2–78 (average = 44) sets of PDF, per sample, and average shock pressures for a given sample were then calculated based on the relative frequencies of these specific orientations as measured. A somewhat similar pressure calibration scheme was proposed by Stöffler and Langenhorst (1994), based on characteristic combinations of PF and PDF orientations; four progressive stages of shock were defined and supported by experimental observations. For example, at pressures of 12–20 GPa, PDF orientations parallel to $\{10\bar{1}3\}$ dominate, while above 20 GPa, PDF orientations parallel to $\{10\bar{1}2\}$ become more abundant.

Based on our study, it appears that in order to reach a minimum level of precision and repeatability, at least 50 PDF sets (better 100 PDF sets) per sample should be measured (Fig. 8). Assuming that the method developed by Grieve and Robertson (1976) is accurate, we estimated the variation in calculated average shock pressures when using the first 25, first 50, and first 100 PDF sets measured. The variation was determined by comparing PDF measurements made by single operators with those based on the compiled group data for that individual sample. Predictably, the most variation, by a factor of ~1.4, was observed when only 25 PDF sets were used from the BOS-3 data. The least variation, by a factor of just ~1.1, was observed when 100 PDF sets were used from the M8-427.7 data.

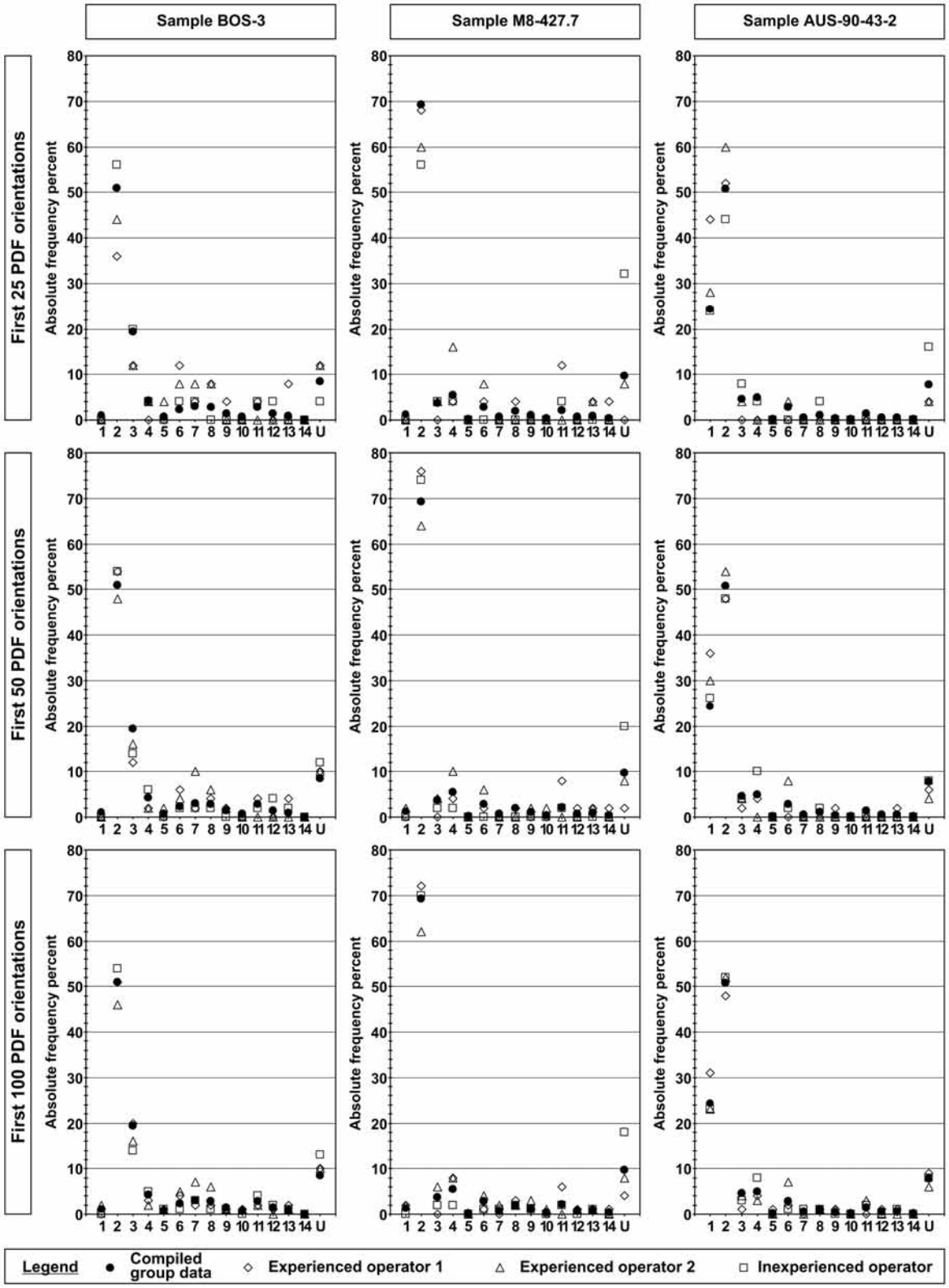

Fig. 8. Absolute frequency distribution of indexed PDFs in quartz grains from BOS-3, M8-427.7, and AUS-90-43-2, as determined by each single operator and compared to the compiled group data (i.e., average of all PDF sets measured by the three operators), which is plotted for reference. Values reported on the x-axis correspond to the different PDF orientations shown in Fig. 1; the relative proportion of unindexed PDF sets (U) is also reported. Only the first 25 measured PDF orientations are reported in the first row, with the first 50 and first 100 measured PDF sets plotted in the second and third rows, respectively.

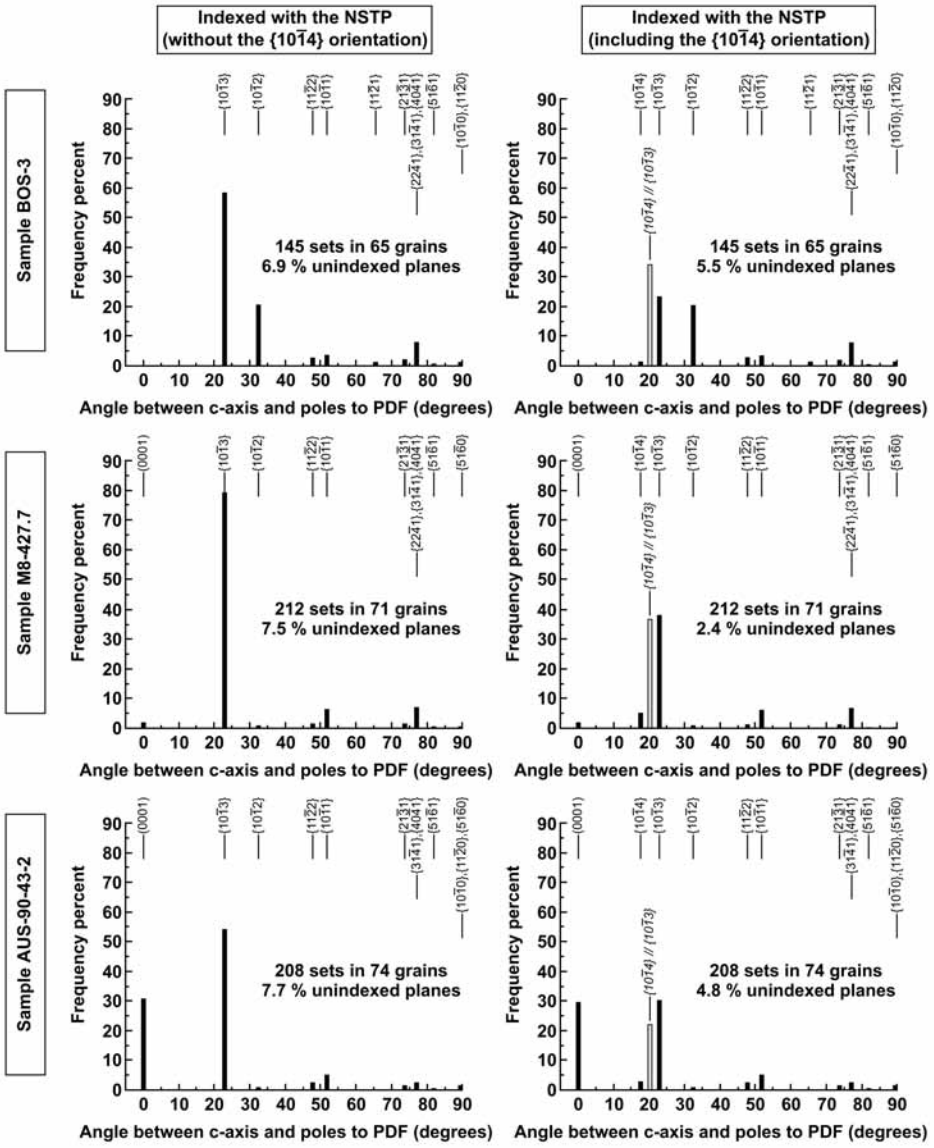

Fig. 9. Histograms of the absolute frequency percent of indexed PDFs in quartz grains from BOS-3, M8-427.7, and AUS-90-43-2, as determined by the experienced operator 1, using two different versions of the NSTP for the indexing, not including (left column) and including (right column) the {10$\bar{1}$4} orientation. Note that PDF planes which plot in the overlapping zone between {10$\bar{1}$4} and {10$\bar{1}$3} crystallographic orientations are shown by gray bars.

We note also that some typical PDF crystallographic orientations in shocked quartz (e.g., {10$\bar{1}$0}, {11$\bar{2}$1}, {21$\bar{3}$1}, {51$\bar{6}$1}, {11$\bar{2}$0}, etc.; see Table 1) are not included in shock barometry calculations, and it is not clear what additional information these higher index sets may potentially provide. Co-existing orientations (such as, e.g., c(0001) and π{10$\bar{1}$2}) in a single quartz grain are also not properly considered in the calculation method of Grieve and Robertson (1976).

CONCLUSIONS AND RECOMMENDATIONS

Our study shows that differences in the abundances of PDF set orientations as measured by different operators are rather limited, both for dominant and for less common "accessory" orientations, when a large number of PDF sets are measured. It seems also that the level of ability of the operator (experienced versus inexperienced) is only responsible for modest differences in the number of unindexed planes. However, a recalculation of the data to 100%, excluding unindexed PDF orientations, reduces the minor influence of operator's ability and permits consistent comparison of the data sets.

The precision of U-stage analysis, which depends mainly on the number of PDF sets investigated, can only be assured by increasing the number of PDF sets measured. When only 25 PDF sets are measured, there is up to a 20 pp variation (or 81%) in the abundances of dominant PDF sets; by measuring 100

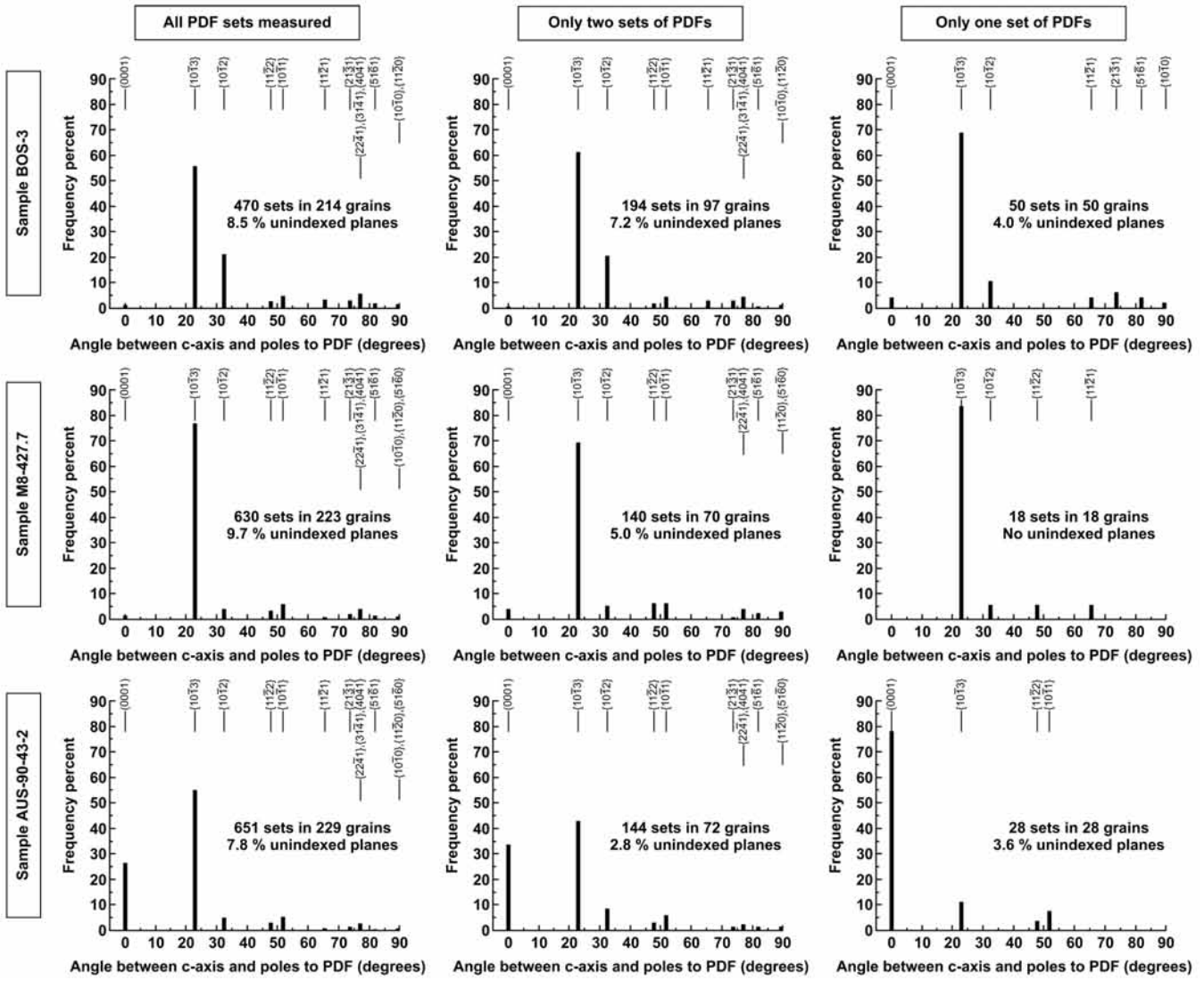

Fig. 10. Histograms of the absolute frequency percent of indexed PDFs (recalculated to 100% without unindexed PDF orientations) in quartz grains from BOS-3, M8-427.7, and AUS-90-43-2. A compilation of all PDF orientations measured by the three operators combined (first column) is compared to histograms based on grains containing only two sets and only one set of PDFs (second and third columns, respectively).

sets, this variation or error can be reduced by nearly two thirds. This finding is especially important when PDF set orientations are being used to calculate shock barometry (cf. Grieve and Robertson 1976). The use of the new stereographic projection template (NSPT; Fig. 1), which includes the positions of five additional typical PDF sets, is recommended, as it may allow indexing of up to 12 pp more PDF planes; these additional PDF sets would remain unindexed using the SPT and potentially regarded as errors of measurement.

On the basis of these results, we conclude that by following a strict measurement procedure, the reproducibility of U-stage data is good and that results can be effectively compared. Further, it is critical that published PDF orientation histograms at least clearly define what frequency measurement is used (i.e., relative or absolute frequency), whether or not unindexed PDF sets are included in the frequency calculations, and the numbers of grains and sets analyzed. This information is essential for comparing datasets from different studies or from different workers examining the same samples. In addition, the relative proportions of each PDF set population, which are combined into the published PDF orientation histograms, should also be reported. This information can be useful for detecting variations in shock within a sample and identifying biases due to methodology.

The universal-stage technique will undoubtedly remain a standard method for the measurement of crystallographic orientations of PDF sets in quartz grains, as it is a relatively fast and inexpensive method of investigation, and is currently the only technique that allows large, statistically useful datasets to be readily generated.

Acknowledgments—This work is supported by the Austrian Science Foundation (FWF), grant P18862-N10, and the Austrian Academy of Sciences. Bevan M. French is gratefully acknowledged for his ongoing assistance with this project. We are grateful to Dieter Stöffler for discussion and encouragement. Jörg Fritz, W. Uwe Reimold, and an anonymous reviewer are also thanked for constructive comments on this manuscript. This paper is dedicated to the memory of Prof. Wolf von Engelhardt (1910–2008), who was one of the pioneers of U-stage measurements of PDFs in shocked quartz grains.

Editorial Handling—Dr. Uwe Reimold

REFERENCES

Alexopoulos J. S., Grieve R. A. F., and Robertson P. B. 1988. Microscopic lamellar deformation features in quartz: Discriminative characteristics of shock-generated varieties. *Geology* 16:796–799.

Bloss F. D. 1971. *Crystallography and crystal chemistry: An introduction*. New York: Holt, Rinehart, and Winston. 545 p.

Bohor B. F., Modreski P. J., and Foord E. E. 1987. Shocked quartz in the Cretaceous-Tertiary boundary clays: Evidence for a global distribution. *Science* 236:705–708.

DeCarli P. S., Bowden E., Jones A. P., and Price G. D. 2002. Laboratory impact experiments versus natural impact events. In *Catastrophic events and mass extinction: Impacts and beyond*, edited by Koeberl C. and MacLeod K. G. Boulder: Geological Society of America, Special Paper 356. pp. 595–605.

Dressler B. O., Sharpton V. L., and Schuraytz B. C. 1998. Shock metamorphism and shock barometry at a complex impact structure: State Islands, Canada. *Contributions to Mineralogy and Petrology* 130:275–287.

Emmons R. C. 1943. The universal stage (with five axes of rotation). *Geological Society of America Memoir* 8. 205 p.

Engelhardt W. v. and Bertsch W. 1969. Shock-induced planar deformation structures in quartz from the Ries crater, Germany. *Contributions to Mineralogy and Petrology* 20:203–234.

Ferrière L., Morrow J. R., Amgaa T., and Koeberl C. 2008. Systematic comparison of universal stage-indexed planar deformation features in quartz: Implications for statistical significance and representation of results (abstract #3010). Large Meteorite Impacts and Planetary Evolution (LMI IV) Meeting, Johannesburg, South Africa, August 17–21, 2008.

French B. M. 1998. *Traces of catastrophe: A handbook of shock-metamorphic effects in terrestrial meteorite impact structures*. LPI Contribution #954. Houston, Texas: Lunar and Planetary Institute. 120 p.

French B. M. and Short N. M., editors. 1968. *Shock metamorphism of natural materials*. Baltimore: Mono Book Corporation. 644 p.

Goltrant O., Cordier P., and Doukhan J.-C. 1991. Planar deformation features in shocked quartz; a transmission electron microscopy investigation. *Earth and Planetary Science Letters* 106:103–115.

Goltrant O., Leroux H., Doukhan J.-C., and Cordier P. 1992. Formation mechanisms of planar deformation features in naturally shocked quartz. *Physics of the Earth and Planetary Interiors* 74:219–240.

Grieve R. A. F. and Robertson P. B. 1976. Variations in shock deformation at the Slate Islands impact structure, Lake Superior, Canada. *Contributions to Mineralogy and Petrology* 58:37–49.

Grieve R. A. F., Coderre J. M., Robertson P. B., and Alexopoulos J. 1990. Microscopic planar deformation features in quartz of the Vredefort structure: Anomalous but still suggestive of an impact origin. *Tectonophysics* 171:185–200.

Grieve R. A. F., Langenhorst F., and Stöffler D. 1996. Shock metamorphism of quartz in nature and experiment: II. Significance in geoscience. *Meteoritics & Planetary Science* 31:6–35.

Gurov E. P. and Gurova E. P. 1991. *Geological structure and rock composition of impact structures*. Kiev: Naukova Dumka Press. 160 p. In Russian.

Gurov E. P., Koeberl C., Reimold W. U., Brandstätter F., and Amare K. 2005. Shock metamorphism of siliceous volcanic rocks of the El'gygytgyn impact crater (Chukotka, Russia). In *Large meteorite impacts III*, edited by Kenkmann T., Hörz F., and Deutsch A. GSA Special Paper 384. Boulder, CO: Geological Society of America. pp. 391–412.

Hörz F. 1968. Statistical measurements of deformation structures and refractive indices in experimentally shock loaded quartz. In *Shock metamorphism of natural materials*, edited by French B. M. and Short N. M. Baltimore: Mono Book Corp. pp. 243–253.

Huffman A. R. and Reimold W. U. 1996. Experimental constraints on shock-induced microstructures in naturally deformed silicates. *Tectonophysics* 256:165–217.

Koeberl C., Reimold W. U., Kracher A., Träxler B., Vormaier A., and Körner W. 1996. Mineralogical, petrographical, and geochemical studies of drill core samples from the Manson impact structure, Iowa. In *The Manson impact structure, Iowa: Anatomy of an impact crater*, edited by Koeberl C. and Anderson R. R. Boulder: Geological Society of America. pp. 145–219.

Langenhorst F. 2002. Shock metamorphism of some minerals: Basic introduction and microstructural observations. *Bulletin of the Czech Geological Survey* 77:265–282.

Morrow J. R. 2007. Shock-metamorphic petrography and microRaman spectroscopy of quartz in upper impactite interval, ICDP drill core LB-07A, Bosumtwi impact crater, Ghana. *Meteoritics & Planetary Science* 42:591–609.

Müller W. F. and Défourneaux M. 1968. Deformationsstrukturen im Quarz als Indikator für Stosswellen: Eine experimentelle Untersuchung an Quartz-Einkristallen. *Zeitschrift für Geophysik* 34:483–504.

Reinhard M. 1931. *Universaldrehtischmethoden*. Basel, Switzerland: Birkhäuser. 118 p.

Robertson P. B. and Grieve R. A. F. 1977. Shock attenuation at terrestrial impact structures. In *Impact and explosion cratering*, edited by Roddy D. J., Pepin R. O., and Merrill R. B. New York: Pergamon Press. pp. 687–702.

Short N. M. and Gold D. P. 1996. Petrography of shocked rocks from the central peak at the Manson impact structure. In *The Manson impact structure, Iowa: Anatomy of an impact crater*, edited by Koeberl C. and Anderson R. R. GSA Special Paper 302. Boulder: Geological Society of America. pp. 245–265.

Stöffler D. and Langenhorst F. 1994. Shock metamorphism of quartz in nature and experiment: I. Basic observation and theory. *Meteoritics & Planetary Science* 29:155–181.

Whitehead J., Spray J. G., and Grieve R. A. F. 2002. Origin of "toasted" quartz in terrestrial impact structures. *Geology* 30:431–434.

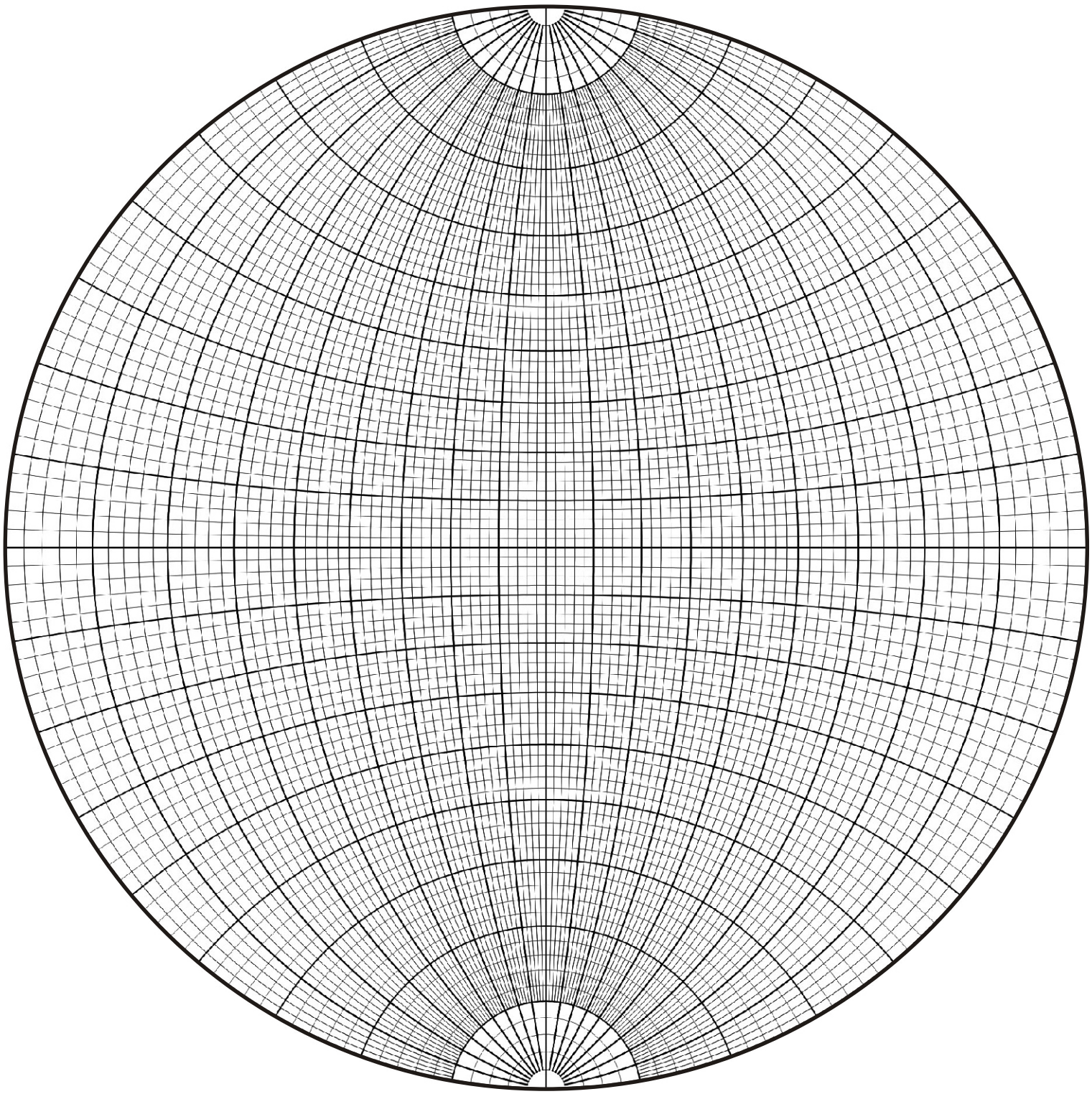

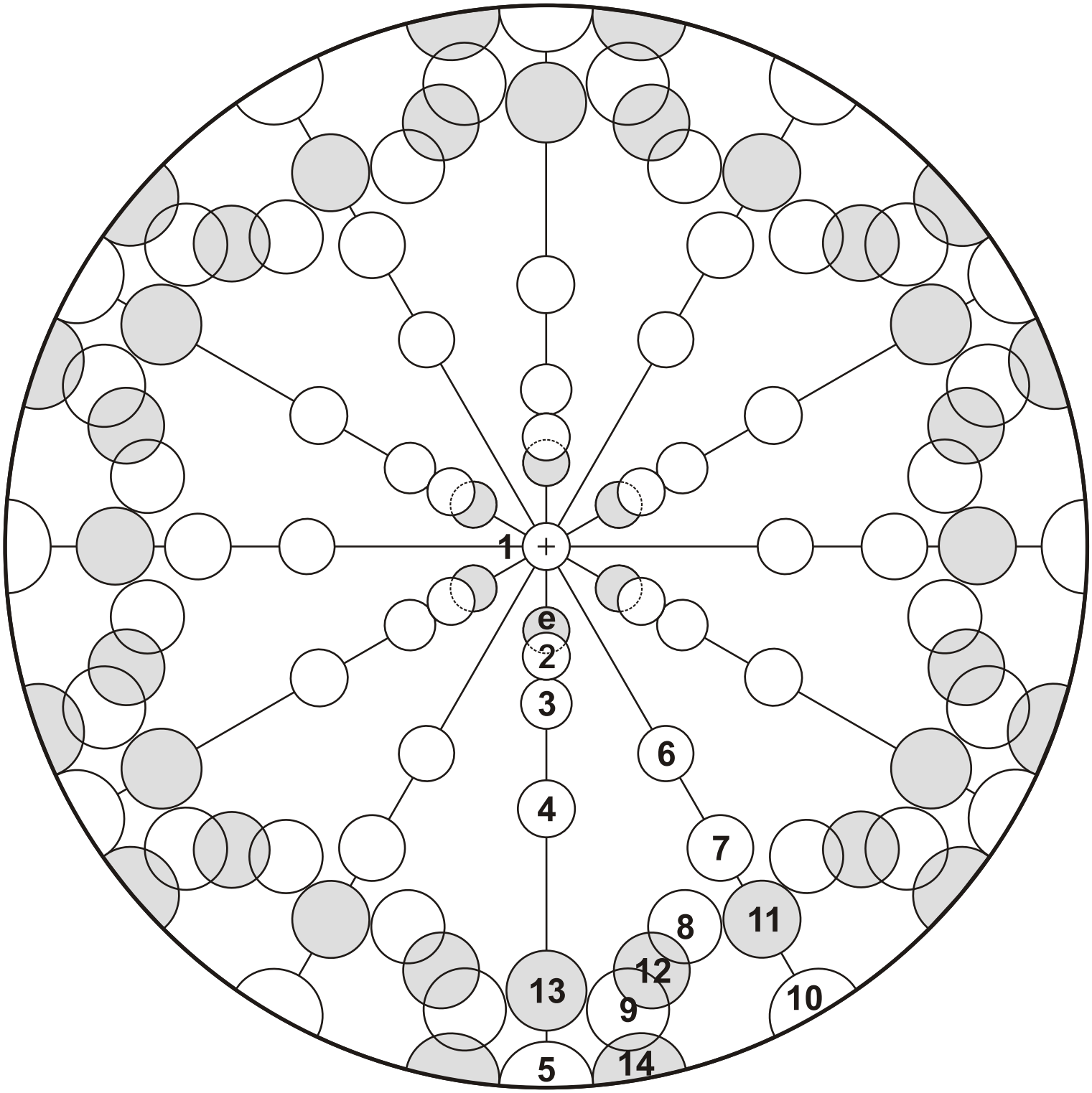

1 (0001) 0.00°
2 {10$\bar{1}$3} 22.95°
3 {10$\bar{1}$2} 32.42°
4 {10$\bar{1}$1} 51.79°
5 {10$\bar{1}$0} 90.00°
6 {11$\bar{2}$2} 47.73°
7 {11$\bar{2}$1} 65.56°
8 {21$\bar{3}$1} 73.71°
9 {51$\bar{6}$1} 82.07°
10 {11$\bar{2}$0} 90.00°
11 {22$\bar{4}$1} 77.20°
12 {31$\bar{4}$1} 77.91°
13 {40$\bar{4}$1} 78.87°
14 {51$\bar{6}$0} 90.00°
e {10$\bar{1}$4} 17.62°